EUROPEAN ORGANIZATION FOR NUCLEAR RESEARCH
CERN – ACCELERATORS AND TECHNOLOGY SECTOR

CERN-ACC-2014-0325

Plasma ignition and steady state simulations of the Linac4 H^- ion source

S. Mattei[1, b)], M. Ohta[2], M. Yasumoto[2], A. Hatayama[2], J. Lettry[1], A. Grudiev[1]

[1]CERN, 1211 Geneva 23, Switzerland

[2]*Graduate school of Science and Technology, Keio University, 3-14-1 Hiyoshi, Kouhoku-ku, Yokohama 223-8522, Japan*

Abstract

The RF heating of the plasma in the Linac4 H^- ion source has been simulated using an Particle-in-Cell Monte Carlo Collision method (PIC-MCC). This model is applied to investigate the plasma formation starting from an initial low electron density of 10^{12} m^{-3} and its stabilization at 10^{18} m^{-3}. The plasma discharge at low electron density is driven by the capacitive coupling with the electric field generated by the antenna, and as the electron density increases the capacitive electric field is shielded by the plasma and induction drives the plasma heating process. Plasma properties such as e^-/ion densities and energies, sheath formation and shielding effect are presented and provide insight to the plasma properties of the hydrogen plasma.

Presented at : 15th International Conference on Ion Sources ICIS13, 9-13 September 2013, Chiba, Japan

Plasma ignition and steady state simulations of the Linac4 H$^-$ ion source [a)]

S. Mattei[1, b)], M. Ohta[2], M. Yasumoto[2], A. Hatayama[2], J. Lettry[1], A. Grudiev[1]

[1]*CERN, 1211 Geneva 23, Switzerland*
[2]*Graduate school of Science and Technology, Keio University, 3-14-1 Hiyoshi, Kouhoku-ku, Yokohama 223-8522, Japan*

(Presented XXXXX; received XXXXX; accepted XXXXX; published online XXXXX)
(Dates appearing here are provided by the Editorial Office)

The RF heating of the plasma in the Linac4 H$^-$ ion source has been simulated using an Particle-in-Cell Monte Carlo Collision method (PIC-MCC). This model is applied to investigate the plasma formation starting from an initial low electron density of 10^{12} m^{-3} and its stabilization at 10^{18} m^{-3}. The plasma discharge at low electron density is driven by the capacitive coupling with the electric field generated by the antenna, and as the electron density increases the capacitive electric field is shielded by the plasma and induction drives the plasma heating process. Plasma properties such as e$^-$/ion densities and energies, sheath formation and shielding effect are presented and provide insight to the plasma properties of the hydrogen plasma.

I. INTRODUCTION

Two ion source prototypes are under development for the new 160 MeV H$^-$ linear accelerator Linac4 at CERN[1]. IS01, a volume source aiming at 0.5 ms pulses of 20 mA H$^-$ current, and IS02, a cesiated source aiming at 40 mA H$^-$ current with fewer co-extracted electrons and a lower emittance. In both ion sources, the plasma is heated by a Radio Frequency (RF) solenoid antenna operated at 2 MHz with a peak power available of 100 kW and a repetition rate of 2 Hz. At each pulse the plasma is newly ignited. In this study we simulate the plasma ignition and the steady state regime for the IS02 prototype via an electromagnetic Particle In Cell Monte Carlo method (PIC-MCC), based on the work of Hayami et al[2]. The real ion source geometry and material properties are taken into account although neglecting the magnetic cusp and filter field.

II. METHOD AND SIMULATION PARAMETERS

The IS02 simulation domain is shown in Fig. 1. The electromagnetic particle-in-cell Monte Carlo method model consists of two parts. One is the 2.5D model of the electromagnetic field (cylindrical symmetric model) and the second is the 3D3V particle dynamics model, where the equations of motion of charged particles are solved numerically in three dimensions. The electric field **E** and the magnetic field **B** are the sum of two contributions. The fields generated by the RF solenoid antenna ($\mathbf{E_{RF}}$ and $\mathbf{B_{RF}}$) are simulated separately by the HFSS software, taking into account the real 3D ion source geometry with its respective material properties[3]. The fields are then averaged in the θ-direction and exported as a field map to the PIC model. The second contribution is the field generated by the plasma itself ($\mathbf{E_{pl}}$ and $\mathbf{B_{pl}}$). This is calculated by solving explicitly Maxwell's equations by the Finite Difference Time Domain (FDTD) method[4], assuming $\partial/\partial\theta = 0$. The two contributions are then summed to give the total electric and magnetic field (i.e. $\mathbf{E} = \mathbf{E_{RF}} + \mathbf{E_{pl}}$). The equations of motion of the charged particles (e$^-$, p$^+$ and H_2^+) are solved numerically in a 3D3V space by the Boris-Buneman method[5] in cylindrical coordinates. The resulting plasma current, which is the sum of the electron and the ion contribution ($\mathbf{j_{pl}} = \mathbf{j_e} + \mathbf{j_i}$), are then averaged in the θ-direction for the 2.5D electromagnetic calculation. Electron collisions with hydrogen atoms, molecules and ions are modeled by the Monte Carlo, Null-Collision method[6]. In the present model Coulomb collisions and ion collisions are not taken into account. Secondary electrons produced by ionization are also tracked while particles reaching the ceramic plasma chamber are lost on the wall and removed from the computation. The neutral gas is taken as a background gas of constant density and a dissociation degree of 10%. The code is parallelized via the MPI interface.

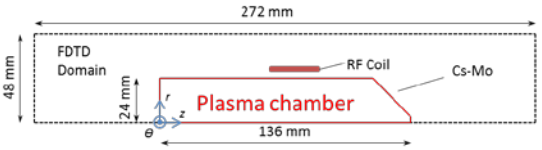

Fig. 1. IS02 simulation domain. The cesiated molybdenum surface facing the plasma is indicated.

[a)]Contributed paper published as part of the Proceedings of the 15th International Conference on Ion Source, Chiba, Japan, September, 2013.
[b)]Author to whom correspondence should be addressed. Electronic mail: stefano.mattei@cern.ch

The assumption of a cylindrical symmetric model does not allow non-homogeneities in the θ-direction to be taken into account. However given the absence of the magnetic cusp and filter field in the present simulations, the fields are expected to be uniform in the θ-direction and therefore well approximated by their average.

The results of two simulation runs are presented. The first represents the plasma ignition from a low initial plasma density of 10^{12} to 10^{16} m^{-3} while the second ranges from 10^{15} m^{-3} to the steady state regime at 10^{18} m^{-3}. The simulation input parameters for the two conditions are summarized in Table I. As initial condition, the charged particles are uniformly distributed in the region $0 \le r \le 12$ mm and $34 \le z \le 102$ mm as indicated in Fig. 2. Plasma neutrality is assumed at the initial condition. From previous simulation results we seed the positive ions as 90% H_2^+ and 10% protons of the electron density. The volume is subdivided uniformly in square cells of 1 mm side. The dimensions of the FDTD domain are taken to be double of the plasma chamber in order to avoid large reflections at the boundary. A time step of 1 ps is chosen, in order to remain below the cyclotron period for electrons. Collisions are evaluated at a larger step interval, each $\Delta t_{coll} = 1.0 \times 10^{-10}$ s. RF parameters are chosen to simulate the Linac4 ion source operated at an antenna current of 70 A, equivalent to 7 kW RF power. The simulation of the ignition phase was performed on 96 parallelized CPUs (eight processors dodeca-cores AMD Opteron 6176 Magny-Cours 2.3 GHz, 4 GB RAM per core). Simulation time was 2 days. The steady state simulation was performed on 192 parallelized CPUs of the same kind, taking 4 days per μs.

TABLE I. Simulation input parameters.

Parameter	Ignition	Steady state
Cell size	1 × 1 mm	1 × 1 mm
Δt	1×10^{-12} s	1×10^{-12} s
Δt_{coll}	1×10^{-10} s	1×10^{-10} s
Particle number	4800	24000
Specific weight	5×10^{4}	1×10^{7}
Initial e^- density	1×10^{12} m^{-3}	1×10^{15} m^{-3}
Frequency	2 MHz	2 MHz
RF power	7 kW	7 kW
Init. e^- temperature	15 eV	15 eV
H_2 pressure	3 Pa	3 Pa
Dissociation degree	10%	10%

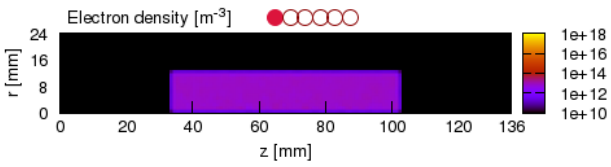

Fig. 2. Initial particle distribution. The RF connection to the solenoid is indicated by the solid red dot.

III. RESULTS

A. Plasma ignition

Plasma ignition was simulated starting from an initial density of 10^{12} m^{-3}. The plasma density as a function of time is shown in Fig. 3. In the period from 0.1 to 0.35μs, the plasma density decreases for half a cycle (0.25μs) and increases during the second half cycle (Fig. 3). Plasma heating takes place by coupling of the RF fields with the charged particles. As shown by Grudiev et al.[3], the $\mathbf{E_{RF}}$ field points primarily in the r and z direction, which causes the electrons to move in the opposite direction to the electric field, leading to a push-pull effect of the electrons during the initial phase, as illustrated in Fig. 4. When the electrons are pushed to the plasma chamber ends greater losses on the wall lead to a decrease in the plasma density. On the contrary, when pulled towards the center electron impact ionization overcomes the losses, and the density increases. This asymmetry is ascribed to the capacitive coupling of the RF field to the plasma (E-mode).

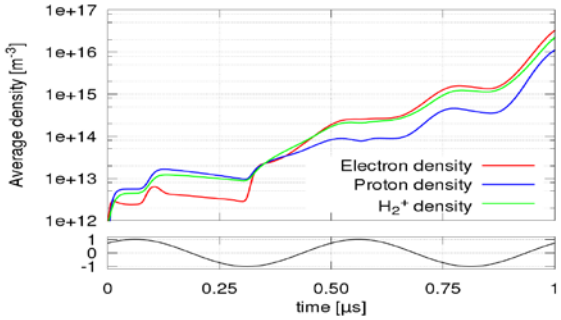

Fig. 3. Plasma density as a function of time during ignition (top). Normalized antenna current (bottom).

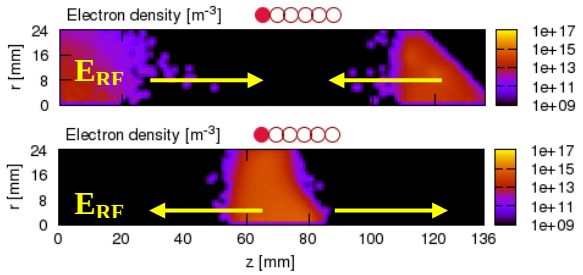

Fig. 4. Electron density distribution at 0.15 μs (top) and 0.4 μs (bottom), corresponding to a RF current phase of π/3 and 4π/3 respectively. At these densities the RF electric field penetrates the plasma region.

At the high voltage connection of the coil (solid red dot in Fig. 4), the ratio of the $\mathbf{E_{RF}}$ components is 16:4:1 in the r, z, θ components respectively. At the low density regime of 10^{12} m^{-3}, $\mathbf{E_{RF}}$ can penetrate the plasma volume to act as the main driving force. When the electron density increases a shielding of the RF electric fields appears. Fig. 5 shows a comparison of the radial component of $\mathbf{E_{RF}}$ at the same phase, but with a different electron density. The higher density effectively shields out the RF field in a sheath located in the region close to the plasma chamber

wall. As the shielding effect takes place the asymmetric behavior previously discussed diminishes, leaving the plasma concentrated in the longitudinal center of the plasma chamber as described in the next section.

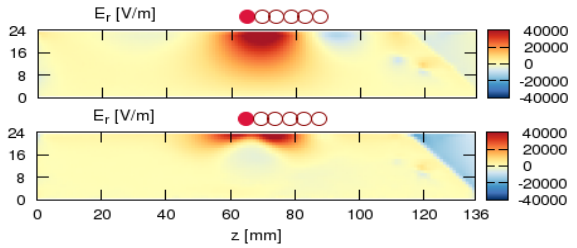

Fig. 5. Radial component of the total electric field $E=E_{RF}+E_{pl}$ for two different electron densities ($5\cdot10^{12}$ m^{-3} top and $5\cdot10^{14}$ m^{-3} bottom) evaluated at the same RF phase of $\pi/3$.

B. Intermediate density to steady state

Starting from an electron density of $10^{15}\,m^{-3}$ the plasma density increases to reach steady state after 1.25 µs at $10^{18}\,m^{-3}$. A clear 4 MHz oscillation of the plasma particle parameters is observed; the increase in the plasma density corresponds to the domination of gas ionization (when the electron energy is sufficient for electron impact ionization) while the density decreases occurs when wall losses dominate. In vacuum, B_{RF} is in phase with the antenna current, while E_{RF} has 90° phase difference. Fig. 6 shows that the electron energy increases for an antenna current of zero, when $\mathbf{E_{RF}}$ is at a maximum.

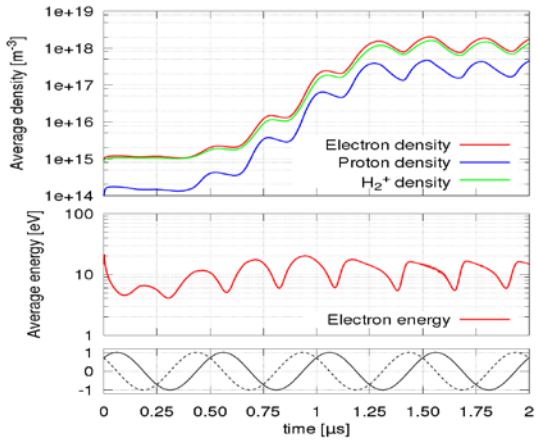

Fig. 6. Average plasma density and electron energy as a function of time for the steady state simulation. The normalized antenna current (solid) and normalized E_{RF} field (dashed) are indicated at the bottom.

A different trend of the electron energy is observed during build-up (first 1.25 µs) and steady state. At steady state a sharper rise is observed, followed by a slower decrease. Also a phase difference appears in the average electron energy. At steady state the minimum of the electron energy is found at a later time compared to the build-up phase. A similar phase shift was observed experimentally in the plasma light emission[8].

Fig. 7 shows a comparison between the electron density distribution at the same RF phase as in Fig. 4 but at a higher electron density. In this steady state regime the plasma shows a quasi-symmetric behaviour, indicating that the heating process is dominated by the inductive mode (H-mode).

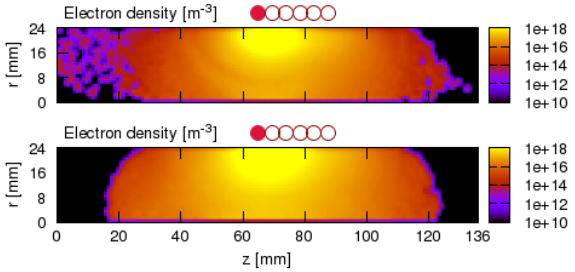

Fig. 7- Electron density distribution at 1.15 µs (top) and 1.4 µs (bottom) corresponding to the start of the steady state and to a RF current phase of $\pi/3$ and $4\pi/3$ respectively.

IV. CONCLUSIONS AND OUTLOOK

We have simulated the plasma ignition and the steady state regime in the Linac4 ion source. First insights into the transition from E to H-mode have been obtained. However the full transition from ignition to steady state still needs to be investigated and will be the subject of further studies. The impact of the multi-cusp and filter field together with further variation of the main simulation parameters (e.g. H_2 pressure, RF power) is foreseen. The electron density and the Electron Energy Distribution Function can be used as input to the Collision-Radiative model that will enable simulation of the photometry observables[7]. As the ultimate goal is the improved production of H^- ions, further improvements will require the implementation of the Monte Carlo model and tracking for neutrals, together with ion collisions and H^- density.

V. REFERENCES

[1] J. Lettry, D. Aguglia, P. Andersson, S. Bertolo, A. Butterworth, Y. Coutron, A. Dallocchio, E. Chaudet, J. Gil-Flores, R. Guida, J. Hansen, A. Hatayama, I. Koszar, E. Mahner, C. Mastrostefano, S. Mathot, S. Mattei, Ø. Midttun, P. Moyret, D. Nisbet, K. Nishida, M. O'Neil, M. Otha, M. Paoluzzi, C. Pasquino, H. Pereira, J. Rochez, J. Sanchez Alvarez, J. Sanchez Arias, R. Scrivens, T. Shibata, D. Steyaert, N. Thaus, T. Yamamoto, *Status and Operation of the Linac4 Ion Source Prototypes*, (these proceedings)

[2] T. Hayami, S. Yoshinari, R. Terasaki, A. Hatayama, and A. Fukano, AIP Conf. Proc. 1390, 339 (2011).

[3] A. Grudiev, J. Lettry, S. Mattei, M. M. Paoluzzi, and R. Scrivens, *Numerical Simulation of Electromagnetic Fields and Impedance of CERN LINAC4 H⁻ Source taking into Account the Effect of the Plasma*, (these proceedings)

[4] K. Yee, *Ant. and Prop., IEEE Transactions on* **14**, 302–307 (1966)

[5] C. Birdsall, and A. Langdon, *Plasma Physics via Computer Simulation*, 2004

[6] K. Nanbu, *Plasma Science, IEEE Transactions on* **28**, 971–990 (2000).

[7] T. Yamamoto, T. Shibata, M. Ohta, M. Yasumoto, K. Nishida, A. Hatayama, S. Mattei, J. Lettry, K. Sawada, and U. Fantz, *Modeling of Neutrals in the Linac4 H- Ion Source Plasma; Hydrogen Atom Production Density Profile and H_α Intensity by CR Model*, (these proceedings)

[8] J. Lettry, Private Communication